Synthesis and Characterization of Conducting Poly(o-aminobenzyl alcohol) and Its Copolymers with Aniline

H. S. O. Chan,* S. C. Ng, W. S. Sim, S. H. Seow, K. L. Tan,† and B. T. G. Tan†

Department of Chemistry, National University of Singapore, Kent Ridge, Singapore 0511, Republic of Singapore

Received June 12, 1992; Revised Manuscript Received October 8, 1992

ABSTRACT: Polyaniline, poly(aniline-*co*-*o*-aminobenzyl alcohol), and poly(*o*-aminobenzyl alcohol) have been synthesized and characterized by a number of techniques including X-ray photoelectron spectroscopy (XPS), ^{1}H nuclear magnetic resonance spectroscopy (^{1}H NMR), thermogravimetry (TG), differential scanning calorimetry (DSC), and ultraviolet–visible absorption spectroscopy (UV–vis). Conductivities of the HCl-doped polymers ranged from 10^1 S cm^{-1} for polyaniline to 10^{-3} S cm^{-1} for poly(*o*-aminobenzyl alcohol). Copolymer compositions show that aniline and *o*-aminobenzyl alcohol have similar reactivities. The substituted polymers exhibited enhanced thermal stability and hydrogen-bonding interactions. The results were rationalized based on the effect of the $-CH_2OH$ substituent on the polymer structure.

Introduction

Electrically conducting organic polymers are a novel class of synthetic metals that combine the chemical and mechanical attributes of polymers with the electronic properties of metals and semiconductors. They breach the traditional view of mutual exclusion between plastics and electrical conductivity, and their development has spurred intense interdisciplinary research in the last 15 years.[1-5]

A wide variety of polyenes, polyaromatics, and polyheterocycles have been investigated in the search for conducting polymers.[6-9] Among these polymers polyaniline has been described as "the conducting polymer for technology".[10] It is relatively inexpensive, readily synthesized by simple procedures, and exhibits good thermal and environmental stability. As a result, polyaniline and its derivatives can be used as an active electrode material,[11,12] in microelectronics,[13,14] and as an electrochromic material.[15,16] The use of substituted polyanilines is mainly to increase the processibility of the polymer, but this approach usually results in a lowering of conductivity.[17-20] Recent methods to improve the processibility of doped polyaniline include the preparation of the polymer in a colloidal form[21] and the careful control of molecular weight by the addition of dianiline in predetermined proportions.[22]

Not all applications require conducting polymers with high conductivity in the region of $10-10^3$ S cm^{-1}. The semiconducting range of $10^{-4}-10^{-1}$ S cm^{-1} can be used as antistatic and EMI shielding materials.[23,24] Our laboratory has been focusing on the preparation and characterization of polymers based on derivatives of aniline for this type of application as well as for the following reasons:

1. They give information on structure–property relations that govern the conductivity and stability of polyaniline.
2. They possess improved processibility.
3. They can act as a basis for the synthesis of new functionalized polymers.
4. They have reduced toxicity as compared to polyaniline.

We report in this paper the chemical syntheses of homopoly(*o*-aminobenzyl alcohol) (POABAL) and its copolymers with aniline. Spectroscopic characterization of the insoluble doped polymers and soluble polymer bases has been carried out by XPS, UV–vis, IR, and NMR techniques. Oxidative thermal stability has been assessed by TG/DSC measurements. We have also been able to determine the compositions of the copolymers by three independent methods.

Experimental Section

Chemicals. Aniline (Aldrich) was distilled and stored under nitrogen in the dark prior to polymerization. Reagent-grade *o*-aminobenzyl alcohol (Aldrich) and sodium peroxodisulfate ($Na_2S_2O_8$; Merck) were used as purchased.

Chemical Preparation of Homopolymers. Polyaniline (PAN) and poly(*o*-aminobenzyl alcohol) (POABAL) were synthesized chemically by oxidative coupling of the monomers in aqueous protonic acid solutions, using $Na_2S_2O_8$ as the initiator.

An aqueous solution of 4.76 g (20 mmol) of $Na_2S_2O_8$ in 50 mL of 1 M HCl was added dropwise, with vigorous stirring, to a 100-mL solution containing 20 mmol of aniline (1.86 g) or *o*-aminobenzyl alcohol (2.46 g) in the same protonic acid medium over a period of 30 min. The temperature of the reaction mixture was maintained at 0–5 °C by an ice bath, and the polymerization was allowed to proceed for 4 h. The pH of the reaction medium was maintained at ~0.1–1.0. The control of temperature is important in the case of POABAL to avoid oxidation of the alcohol to the acid. The polymer powder formed was filtered under suction, rinsed with ca. 100 mL of the cold corresponding acid, and dried under dynamic vacuum for 24 h to yield the corresponding conducting polymer salt.

The homopolymer bases were prepared by stirring the freshly filtered polymer salts in 100 mL of 0.1 M aqueous NaOH at 0–5 °C for 2 h. The powders were filtered off under suction, rinsed with cold deionized water until the pH of the filtrate was ~7, and dried under dynamic vacuum for 24 h.

Preparation of Copolymers. Three poly(aniline-*co*-*o*-aminobenzyl alcohol) copolymers (PANAL) with different comonomer feed ratios were synthesized chemically in an analogous manner to the homopolymers using HCl as the acid medium. Experimental details are provided in Table I.

Elemental Analysis. The polymer samples were analyzed by the Microanalytical Laboratory using a Perkin-Elmer Model 2400 C, H, N analyzer. The chlorine and sulfur contents were determined by the oxygen flask method.

X-ray Photoelectron Spectroscopy. The vacuum-dried polymer powders were mounted onto a VG sample holder using double-sided adhesive tape. Core-level spectra were obtained on a VG ESCA/SIMSLAB MK II spectrometer with a Mg Kα radiation source (1253.6 eV). All binding energies were referenced to the peak in the C 1s envelope, defined at 285.0 eV, to compensate for surface charging effects. Spectral deconvolution was carried out using Gaussian component peaks with constant full widths at half-maximum (fwhm) for all components in a

* To whom correspondence should be addressed.
† Department of Physics, National University of Singapore.

0024-9297/93/2226-0144$04.00/0

Table I
Experimental Details for the Copolymerization of o-Aminobenzyl Alcohol

sample	aniline	o-aminobenzyl alcohol	feed ratio aniline: o-aminobenzyl alcohol	mole fraction of o-aminobenzyl alcohol in feed
PANAL21	1.24 g (13.3 mmol)	0.82 g (6.7 mmol)	2:1	0.33
PANAL11	0.93 g (10.0 mmol)	1.23 g (10.0 mmol)	1:1	0.50
PANAL12	0.62 g (6.7 mmol)	1.64 g (13.3 mmol)	1:2	0.67

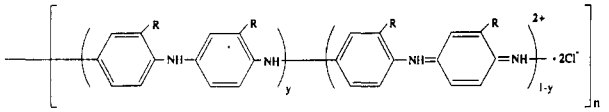

Figure 1. General structure of the copolymer.

particular spectrum. Surface elemental stoichiometries were obtained from peak area ratios corrected with the appropriate experimentally determined sensitivity factors and are subjected to ±10% error.

Thermogravimetry. The polymers were subjected to oxidative thermal degradation studies on a Du Pont Thermal Analyst 2100 system with a TGA 2950 thermogravimetric analyzer module. The analyses were carried out from room temperature to 750 °C at a linear heating rate of 10 °C min^{-1} and a dynamic air flow of 75 cm^3 min^{-1}. Finely divided samples of about 10 mg were used.

Differential Scanning Calorimetry. DSC studies of the polymers were performed on a Du Pont Thermal Analyst 2100 system with a DSC 2910 module. The analyses were carried out from room temperature to 350 °C at a linear rate of 10 °C min^{-1}. Nitrogen at a flow rate of 75 cm^3 min^{-1} acted as the purge gas. Finely divided samples of about 5 mg were used.

Infrared Spectroscopy. IR spectra of the polymer bases were recorded on a Shimadzu IR-470 infrared spectrophotometer. The spectra were measured at room temperature (30 °C), with the polymer samples dispersed in KBr disk pellets.

Nuclear Magnetic Resonance Spectroscopy. ^1H NMR spectra of the polymer bases were recorded on a Bruker ACF 300 FT-NMR spectrometer operating at 300 MHz. Deuterated dimethyl sulfoxide (DMSO-d_6) was used as solvent and tetramethylsilane (TMS) as an internal reference. Dilute solutions of the polymers (~1% w/v) were used to ensure maximum dissolution.

Ultraviolet–Visible Absorption Spectroscopy. UV–vis solution spectra of the polymer bases were measured on a Hewlett Packard Model 8452A diode array spectrophotometer. The cell temperature was maintained at 25 °C by a Hewlett Packard Model 8909A temperature control unit. Dilute solutions of the polymers in *N*-methyl-2-pyrrolidone (NMP) were used.

Electrical Conductivity Measurement. Conductivity measurements were carried out on a four-point probe connected to a Keithley voltmeter constant-current source system. The polymers tested were in the form of compacted disk pellets 12.7 mm in diameter and ~0.5 mm in thickness. Conductivities were calculated based on the average of at least 10 pairs of consistent readings taken at different points on the pressed pellet.

Results and Discussion

The general structure of the homo- and copolymer salt is given in Figure 1 where R = H or CH_2OH depending on the polymer composition and *y* varies from 0 to 1 with the oxidation state of the polymer. The bulk elemental compositions of the chemically prepared polymers are shown in Table II. The carbon content is slightly higher than that predicted theoretically, and this is probably due to the presence of oligomers and oxidation and degradation products which are not removed by the washing process. The hydrogen content, especially in the polymer salts, are much higher than expected. This can be attributed to water molecules bound to the polymers which are not extracted by vacuum drying, as well as moisture that is absorbed by the dopants during the handling of the polymers under high relative humidity conditions (>70%).

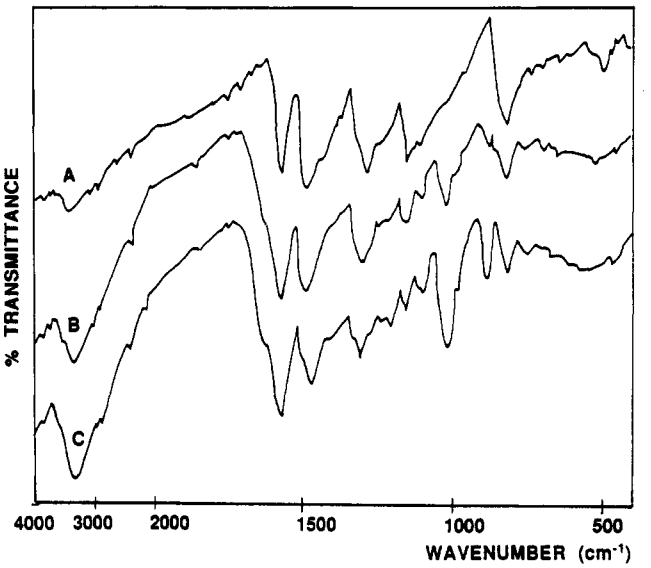

Figure 2. IR spectra of (A) Pan–Base, (B) PANAL11–Base, and (C) POABAL–Base.

Table II
Surface and Bulk Stoichiometries and Conductivities of Homo- and Copolymers

polymer	atomic ratios found in bulk atomic ratio found on surface (XPS) (atomic ratios expected)	conductivities (S cm^{-1})
PAN–HCl	$C_{6.19}H_{7.60}N_{1.00}Cl_{0.47}S_{0.14}$	
	$C_{8.32}O_{0.50}N_{1.00}Cl_{0.41}S_{0.01}$	1.4×10^{1}
	$(C_{6.00}O_{0.00}H_{5.00}N_{1.00}Cl_{0.50}S_{0.00})$	
PANAL21–HCl	$C_{6.77}H_{8.01}N_{1.00}Cl_{0.46}S_{0.10}$	
	$C_{8.03}O_{0.93}N_{1.00}Cl_{0.33}S_{0.01}$	6.6×10^{-2}
	$(C_{6.33}O_{0.33}H_{5.67}N_{1.00}Cl_{0.50}S_{0.00})$	
PANAL11–HCl	$C_{7.16}H_{8.26}N_{1.00}Cl_{0.42}S_{0.17}$	
	$C_{7.89}O_{1.31}N_{1.00}Cl_{0.30}S_{0.11}$	2.2×10^{-3}
	$(C_{6.50}O_{0.50}H_{6.00}N_{1.00}Cl_{0.50}S_{0.00})$	
PANAL12–HCl	$C_{7.40}H_{8.65}N_{1.00}Cl_{0.33}S_{0.22}$	
	$C_{8.43}O_{1.55}N_{1.00}Cl_{0.21}S_{0.12}$	1.6×10^{-3}
	$(C_{6.67}O_{0.67}H_{6.33}N_{1.00}Cl_{0.50}S_{0.00})$	
POABA–HCl	$C_{7.75}H_{8.94}N_{1.00}Cl_{0.47}S_{0.07}$	
	$C_{10.6}O_{2.14}N_{1.00}Cl_{0.35}S_{0.04}$	1.4×10^{-3}
	$(C_{7.00}O_{1.00}H_{7.00}N_{1.00}Cl_{0.50}S_{0.00})$	

The IR spectra of the PAN–Base, PANAL 11–Base, and POABAL–Base are shown in Figure 2. All three bases show a broad absorption band centered between 3300 and 3400 cm^{-1} due to the overlap of N–H and O–H stretching vibrations. The quinoid and benzenoid stretchings at 1580 and 1480 cm^{-1}, respectively,[25] are about 10 cm^{-1} lower than expected, indicating a certain degree of residual doping in the polymer bases.[26] The relative intensities of these bands are a measure of the oxidation state of the polymer. It is thus evident that under identical polymerization times, introduction of the $-CH_2OH$ group increases the level of oxidation. This is further supported by the significance of the C=N stretching shoulder at 1630 cm^{-1}.[27] The most important trend, however, is the emergence and increasing intensity of the band at 1010 cm^{-1} with increasing substitution. On the basis of the spectrum of benzyl alcohol,[28] this has been attributed to the C–O stretching of the alcohol side chain. The absence of any detectable

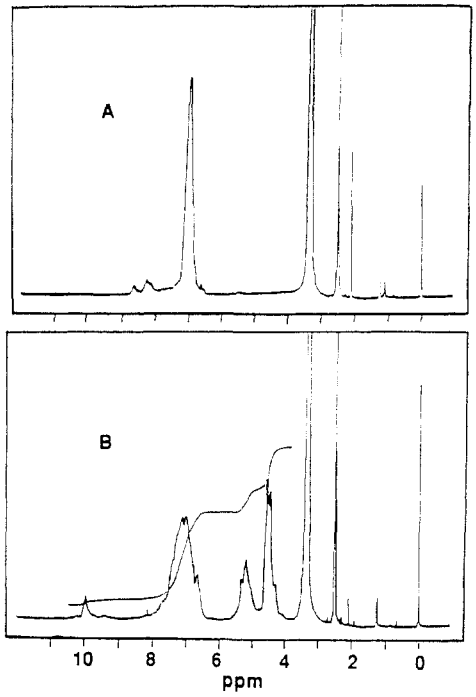

Figure 3. ^{1}H NMR spectra of (A) PAN–Base and (B) POABAL–Base in DMSO-d_6.

C=O stretching absorptions suggests that negligible side-chain oxidation has occurred.

The substitution patterns of the aromatic rings can be deduced from the C–H in-plane and out-of-plane bending bands in the region 750–1100 cm^{-1}.[25] Absorptions at 1100 and 820 cm^{-1} (PAN–Base) suggest 1,4-disubstitution, while those at 1100, 880, and 810 cm^{-1} (POABAL–Base) indicate predominantly 1,2,4-trisubstitution.

^{1}H NMR spectra of PAN–Base and POABAL–Base are shown in Figure 3. PAN–Base has a multiplet peak at 6.6–7.4 ppm which has been assigned to aromatic[29] and amine protons.[30] The correspoonding multiplets in POABAL–Base are spread over a wider range (6.5–8.0 ppm), in accordance with the deshielding of the aromatic protons by the inductive effect of the CH_2OH group. For the substituted polymers, the triplet at 5.16 ppm (removed by addition of D_2O) and the doublet at 4.49 ppm are assigned to the hydroxyl and methylene protons in the side chain, respectively. In addition, a very small peak at 9.94 ppm due to the aldehydic proton is observable, which arises as a result of side-chain oxidation during the polymerization process. It should also be noted that carboxylic protons, which may also be formed, are not detectable by NMR spectroscopy due to the base treatment of the polymers. The integrated intensities for POABAL–Base are close to the expected value of 3.5:1:2 for aromatic and amine: hydroxyl:methylene protons, suggesting that side-chain oxidation is minimal.

UV–vis solution spectra of the polymer bases in NMP are shown in Figure 4. The spectra all consist of two major absorption bands. The first band at 320–328 nm (3.87–3.78 eV) is assigned to the π–π^* transition based on earlier studies on polyaniline[31] and is related to the extent of conjugation between phenyl rings in the polymer chain. It exhibits a hypsochromic shift from 328 nm (3.78 eV) for PAN–Base to 320 nm (3.87 eV) for POABAL–Base, implying a decrease in the extent of conjugation and an increase in the bandgap. This can be attributed to the possible steric repulsion between the bulky $-CH_2OH$ groups and hydrogens on adjacent phenyl rings, which causes the increase in the torsional angles between the rings so as to relieve the steric strain.

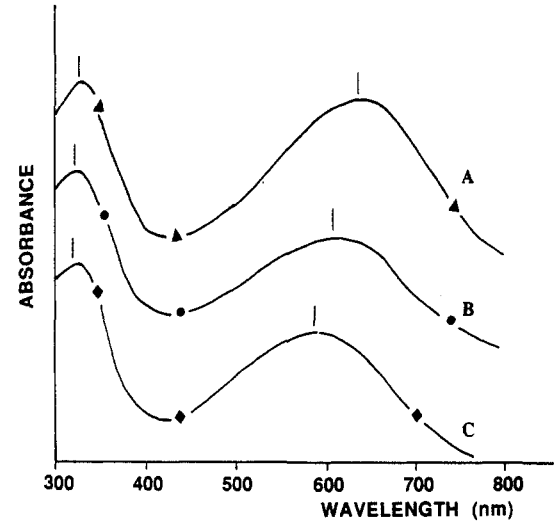

Figure 4. UV–vis spectra of (A) PAN–Base, (B) PANAL11–Base, and (C) POABAL–Base.

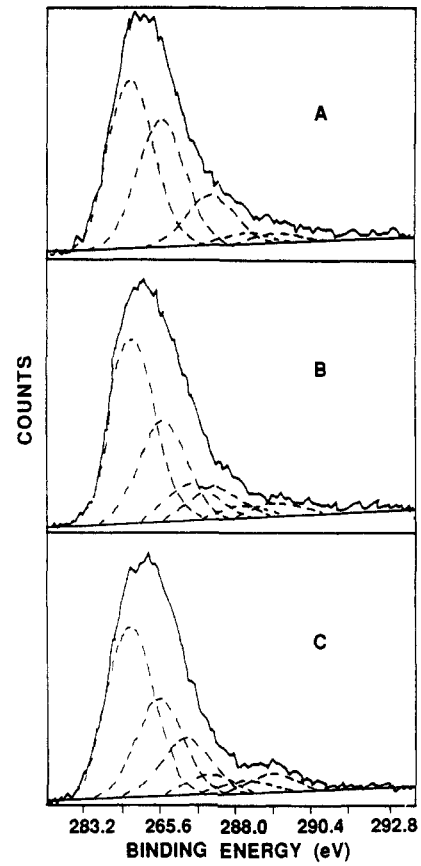

Figure 5. C 1s XPS spectra of (A) PAN–HCl, (B) PANAL11–HCl, and (C) POABAL–HCl.

The second absorption band is assigned to the "exciton" transition caused by interchain or intrachain transfer.[32] This band has been found to be sensitive to the overall oxidation state of the polymer.[33,34] It shows a hypsochromic shift from 636 nm (1.95 eV) in PAN–Base to 584 nm (2.12 eV) in POABAL–Base, implying an increase in the oxidation state of the polymer with increasing substitution, in good agreement with IR results.

XPS core level spectra for C 1s, N 1s, and C 12p are shown in Figures 5–7 respectively. The surface stoichiometries of the polymers which have been determined from elemental peak areas corrected by the appropriate sensitivity factors are shown in Table II. While the chlorine and sulfur contents agree reasonably well with the elemental analysis results, the carbon content appears

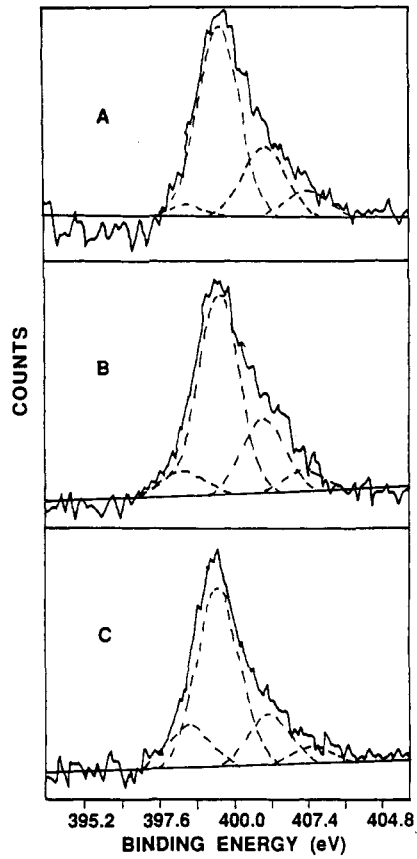

Figure 6. N 1s XPS spectra of (A) PAN-HCl, (B) PANAL11-HCl, and (C) POABAL-HCl.

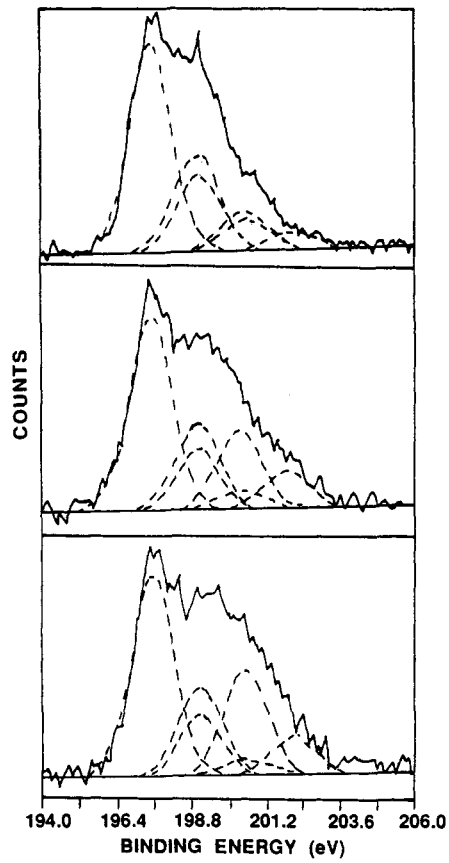

Figure 7. C 1s p XPS spectra of (A) PAN-HCl, (B) PANAL11-HCl, and (C) POABAL-HCl.

to be exceedingly high. This has been attributed mainly to hydrocarbon contamination of the surface which occurs invariably in any XPS analysis.[35] Higher than expected oxygen contents are also observed, and this is probably due to contributions from bound water, polymer hydrolysis, and residual oxidant.[36]

Table III
Quantitative Area Ratio Analysis of C 1s Peak Components

polymer	*C*-N$^+$ (288.3 eV)/ *C*-N (285.6 eV)	*C*-O (286.3 eV)/ *C*-N (285.6 eV)	O*C*=O (289.2 eV)/ *C*-N (285.6 eV)
PAN-HCl	0.33	0.00	0.00
PAN21-HCl	0.27	0.17	0.01
PAN11-HCl	0.29	0.25	0.01
PAN12-HCl	0.27	0.31	0.01
POABA-HCl	0.23	0.45	0.05

The C 1s envelopes of the polymers have a similar shape, with a tail toward the high binding energy indicative of the long-range disordered conjugation present. On the basis of previous XPS studies on polymers,[35,37] the C 1s peak can be deconvoluted into six environments: *C*-C or *C*-H (284.6 eV); *C*-N or *C*=N (285.6 eV); *C*-O (286.5 eV); *C*-N$^{\bullet+}$ (287.2 eV); *C*-N$^+$ (288.3 eV) and O*C*=O (289.2 eV). By assuming that the hydrocarbon contamination only affects the peak at 284.6 eV and correcting for the area of the 289.2 peak due to the absorption tail (by a subtraction of the corresponding percentage peak area of PAN synthesized under similar conditions), the peak areas for the carbon environments can be used to calculate their relative atomic ratios. The results are presented in Table III. The extent of side-chain oxidation to the carboxyl group has been estimated to be less than 10% for the majority of the polymers.

The N 1s spectra of the polymer bases consist of a symmetrical peak. On protonic acid doping, the line width is reduced and a high-binding-energy shoulder appears.[38] The peak can be deconvoluted into four environments as follows: -N= (398.5 eV); -NH- (399.7 eV); -$^{\bullet+}$NH- (401.2 eV) and -$^+$NH$_2$- (402.5 eV). The first two assignments are made based on previous XPS studies on leucoemeraldine and emeraldine base,[35] while titration[39] and secondary ion mass spectrometry[40] on polyaniline have confirmed protonation of both nitrogen species.

It can be seen from Table IV that, for the doped polymer salts, the total proportion of positively-charged nitrogen (N$^+$) is inversely proportional to the amount of *o*-aminobenzyl alcohol in the copolymer. This lowering in the degree of doping is believed to have a detrimental effect on the conductivity of the polymer. Analysis of the total imine:amine ratio confirms the oxidation level state variation as found in the IR studies.

The C 2p spectra can be resolved into three spin-orbit doublets (Cl 2p$_{3/2}$ and Cl 2p$_{1/2}$) separated by 1.5 eV with an area ratio of 2:1. The Cl 2p$_{3/2}$ peaks lie at 197.5, 199.0, and 200.5 eV and are assigned to imine ionic Cl$^-$, amine ionic Cl$^-$, and covalent -Cl from ring substitution or molecular HCl, respectively.[41] Ring substitution via 1,4-addition of HCl to oxidized quinoid units has recently been substantiated by studies on pernigraniline base.[42] The S 2p spectra show a peak centered at 169.0 eV which is characteristic of a sulfate environment SO_4^{2-} or HSO_4^-.[43] It is important to note that significant amounts of residual sulfur from the oxidant are detected in the HCl-doped polymers. No attempt was made to rationalize the O 1s spectra due to the uncertainty in the nature of the oxygen environments.

The total anion (Cl$^-$ + S):N$^+$ ratio is approximately 1:1 for the chemically synthesized polymers, indicating that sulfur exists predominantly as HSO_4^- so as to maintain charge balance. This balance suggests the localization of unit positive charge on the protonated nitrogen and is consistent with the concept of polyaniline being a nitrogenonium ion polymer.[44]

Table IV
Quantitative Area Ratio Analysis of N 1s, Cl 2p, and S 2p Peak Components

polymer	N^+ (401.2, 402.5 eV)	–N= (298.5 eV)	–NH– (399.7 eV)	Cl^- (197.5, 199.0 eV)	–Cl (200.5 eV)	$(Cl^- + S)/N^+$
PAN–HCl	0.34	0.04	0.63	0.88	0.12	1.12
PANAL21–HCl	0.28	0.07	0.65	0.84	0.16	1.04
PANAL11–HCl	0.31	0.08	0.61	0.75	0.25	1.10
PANAL12–HCl	0.27	0.06	0.67	0.66	0.34	0.95
POABA–HCl	0.24	0.15	0.61	0.71	0.29	1.01

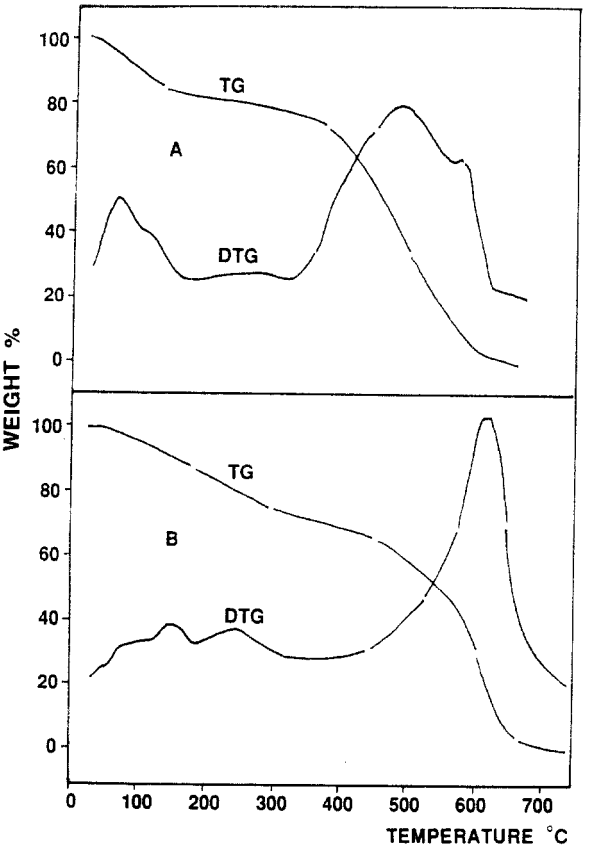

Figure 8. TG curves of (A) PAN–HCl and (B) POABAL–HCl in air.

TG curves for the polymers PAN–HCl and POABAL–HCl are shown in Figure 8. The thermal degradation can be roughly divided into three main weight-loss steps.[45-47] The first weight loss from room temperature to ca. 190 °C (for polymer salts) and ca. 150 °C (for polymer bases) is due primarily to the expulsion of absorbed water and free acid from the polymer matrix. The second weight loss from 190 to 350 °C has been attributed to the loss of the acid dopant. The undoped POABAL–Base also experiences a weight change at this temperature range, suggesting that some simultaneous elimination process also occurs in the substituted polymers. This is likely to be the decomposition or rearrangement of the side chain. The third weight loss from 350 to 700 °C is caused by the oxidative thermal breakdown of the polymer backbone. It is interesting to note that both the onset of this final step and the temperature of maximum rate of decomposition are about 50–100 °C higher for POABAL as compared to PAN.

The enhanced stability of POABAL may be rationalized by the proposed structure shown in Figure 9. Adjacent $-CH_2OH$ units undergo a heat-induced condensation, expelling water and forming ether cross-linkages, which stabilize the polymer against oxidative thermal decomposition.

DSC curves of the same two polymers are shown in Figure 10. It is of great interest to note the very different modes of thermal responses between the two polymers.

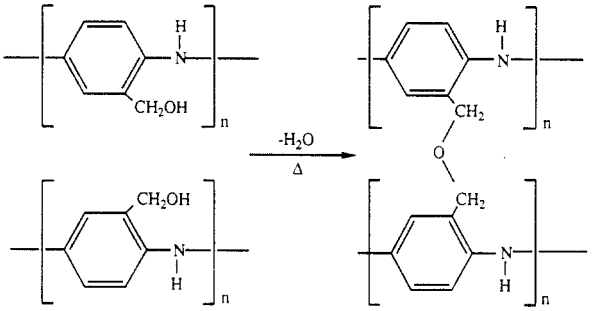

Figure 9. Condensation reaction to form an ether linkage between polymer chains.

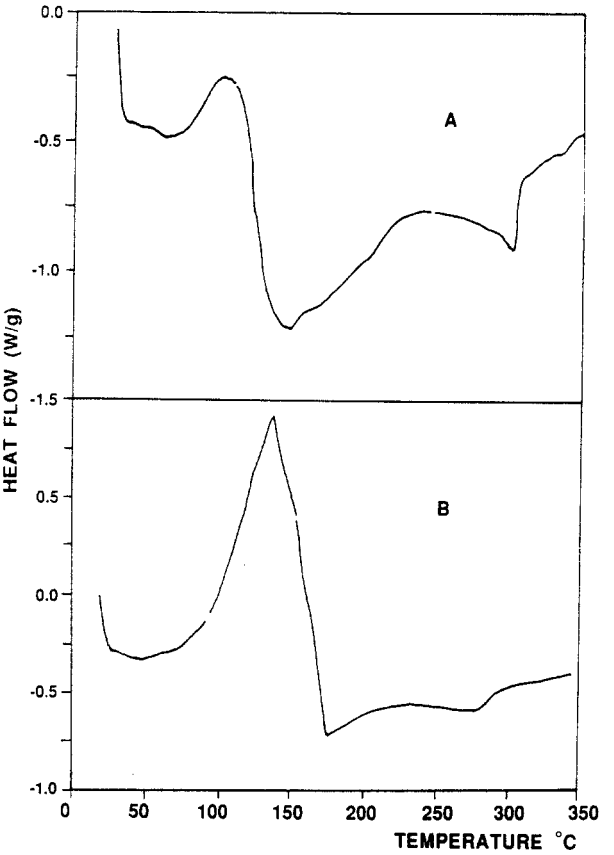

Figure 10. DSC curves of (A) PAN–HCl and (B) POABAL–HCl.

PAN–HCl shows a broad endothermic peak of energy 192.3 J g^{-1} at 140–190 °C corresponding to the elimination of water and acid dopant, as well as an endothermic peak at ca. 280 °C which was previously assigned to a maorphological change in the polymer.[48] POABAL–HCl, on the other hand, exhibits an exotherm between 100 and 175 °C which is likely to be a composite of a number of events: the exothermic inter- and intramolecular hydrogen bonding in POABOL as shown in Figure 11; the energy required to expel the H_2O; and the possible evolution of energy due to new ether bond formation. More work is needed to resolve the different processes to determine the temperature at which they occur and the nature of the competing overlapping transitions. An endotherm is also observed

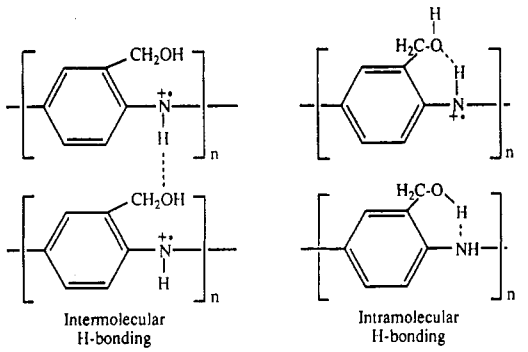

Figure 11. Proposed mechanism for H-bonding in POABAL.

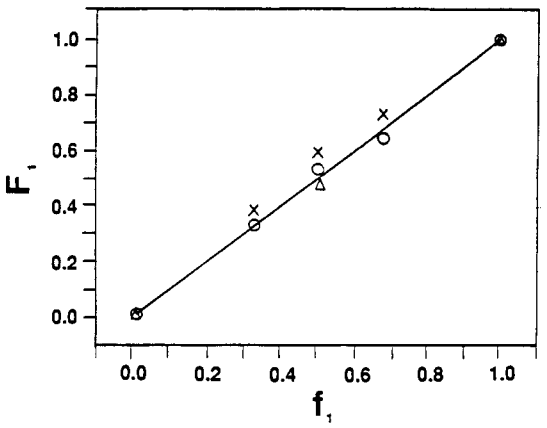

Figure 12. Plot of F_1 against f_1 (×, microanalysis; ○, XPS; △, NMR).

around 250–275 °C. This can be attributed to morphological changes described earlier for PAN–HCl within the polymer matrix although no visual changes were detected under the hot-stage microscope. No T_g base-line shift was observed in the present samples although Wei et al.[49] recently reported T_g in the range of ~105–200 °C for a PAN–base film containing ~0–16% of NMP.

It is well established that, for many copolymers, the composition is different from that based on the monomer feed and is dependent on the reactivity ratio of the monomers. The determination of this copolymer composition is important to see how each component affects the overall properties. In the present work, the copolymer composition F_1 (defined as the mole fraction of *o*-aminobenzyl alcohol units in the copolymers) has been determined by three independent methods: (1) XPS (from the ratio of *C*–O + *C*=O to *C*–N); (2) microanalysis (from the fraction of excess C after correction for contamination by the linear interpolation method); (3) ^{1}H NMR (from the ratio of the peak area of methylene + hydroxyl to aromatic + amine protons).

The relationship between F_1 and the feed composition f_1 (defined as the mole fraction of *o*-aminobenzyl alcohol units in the monomer feed) is shown in Figure 12. All the points lie close to the diagonal line $F_1 = f_1$, suggesting similar monomer reactivities for both aniline and *o*-aminobenzyl alcohol. The results are consistent with the proposed mechanism for the polymerization of aniline and its derivatives,[50] which involves the formation of aniline dimers (rate determining) and subsequent growth of the polymer chain via an electrophilic substitution reaction. While the steric effect of the $-CH_2OH$ group may hinder the initial step, the dimers once formed undergo coupling with the monomers depending on their reactivities toward electrophilic substitution, which are governed by electronic factors. The CH_2OH group is only slightly electron withdrawing by a secondary inductive effect ($\sigma_I = +0.10$).[51] As such, the reactivity of *o*-aminobenzyl alcohol toward electrophilic substitution should not differ greatly from that of aniline. This conclusion is in agreement with the experimental results.

Conclusion

Conducting homopolymers and copolymers based on aniline and *o*-aminobenzyl alcohol have been synthesized chemically. Characterization of the polymers by a host of techniques supports their proposed structures and shows that negligible oxidation of the side chain occurs under the described experimental conditions. The decrease in conductivities is due mainly to the steric effect of the $-CH_2OH$ substituent which lowers the conjugation as indicated by the hypsochromic shifts in the π–π^* transition in the UV–vis spectra. This is supported by the XPS results which show that the total proportion of positively-charged nitrogen (N^+) varies from 34% for the most conducting PAN–HCl homopolymer to 24% for the least conducting POABAL. The NMR shifts, the proposed hydrogen-bonding interactions, and the copolymerization behavior can be attributed to the electronic effect of the $-CH_2OH$ group. The significant increase in thermal stability is a direct result of the intermolecular interactions induced by the substituent group.

References and Notes

(1) Kanatzidis, M. G. *Chem. Eng. News* **1990**, *68*, 36.
(2) Reynolds, J. R. *CHEMTECH* **1988**, *18*, 440.
(3) Greene, R. L.; Street, G. B. *Science* **1984**, *226*, 651.
(4) Naarmann, H. *Adv. Mater.* **1990**, *2*, 345.
(5) Roth, S.; Filzmoser, M. *Adv. Mater.* **1990**, *2*, 356.
(6) Chaing, C. K.; Druy, M. A.; Gau, S. C.; Heeger, A. J.; Lewis, E. J.; MacDiarmid, A. G.; Park, Y. W. *J. Am. Chem.* **1978**, *100*, 1013.
(7) Lin, J. W. P.; Dudek, L. P. *J. Polym. Sci., Polym. Lett. Ed.* **1980**, *18*, 2869.
(8) Diaz, A. F.; Kanazawa, K. K.; Gardini, G. P. *J. Chem. Soc., Chem. Commun.* **1979**, 635.
(9) de Surville, R.; Jozefowicz, M.; Yu, L. T.; Perichon, J.; Buvet, R. *Electrochem. Acta* **1968**, *13*, 1451.
(10) Epstein, A. J.; MacDiarmid, A. G. *Faraday Discuss. Chem. Soc.* **1989**, *88*, 317.
(11) Oyama, N.; Ohsaka, T. *Synth. Met.* **1987**, *18*, 191.
(12) Noufi, R.; Nozik, A. J.; White, J.; Warren, L. F. *J. Electrochem. Soc.* **1982**, *129*, 2261.
(13) Paul, E. W.; Ricco, A. J.; Wright, M. S. *J. Phys. Chem.* **1985**, *89*, 1441.
(14) Chao, S.; Wrighton, M. S. *J. Am. Chem. Soc.* **1987**, *109*, 6227.
(15) Katani, A.; Yano, J.; Sasaki, K. J. *J. Electroanal. Chem.* **1986**, *209*, 227.
(16) Watanabe, A.; Mori, K.; Iwasaki, Y.; Nakamura, Y. *Macromolecules* **1987**, *20*, 1793.
(17) Lacroix, J. C.; Garcia, P.; Audiere, J. P.; Clement, R.; Kahn, O. *Synth. Met.* **1991**, *44*, 117.
(18) Wei, Y.; Focke, W. W.; Wnek, G. E.; Ray, A.; MacDiarmid, A. G. *J. Phys. Chem.* **1989**, *93*, 495.
(19) Oka, O.; Kiyohara, O.; Yoshino, K. *Jpn. J. Appl. Phys.* **1991**, *30*, L653.
(20) Wang, S.; Wang, F.; Ge, X. *Synth. Met.* **1986**, *16*, 99.
(21) Armes, S. P.; Aldissi, M. *U.S. Patent* 4,959,180, 1990.
(22) Cameron, R. E.; Clement, S. K. *U.S. Patent* 5,008,041, 1991.
(23) Duke, C. B.; Gibson, H. W. *Kirk-Othmer: Encyclopedia of Chemical Tochnology*; John Wiley and Sons, Inc.: New York, 1982; Vol. 18, p 755.
(24) *Mod. Plast. Int.* **1982**, Sept, 46.
(25) Tang, J.; Jing, X.; Wang, B.; Wang, F. *Synth. Met.* **1988**, *24*, 231.
(26) Ohira, M.; Sakai, T.; Takeuchi, M.; Kobayashi, Y. *Synth. Met.* **1987**, *18*, 347.
(27) Ohsaka, T.; Ohnuki, Y.; Oyama, N.; Katagiri, G.; Kamisako, K. *J. Electroanal. Chem.* **1984**, *161*, 39.
(28) Silverstein, R. M.; Bassler, G. C.; Morill, T. C. *Spectrometric Identification of Organic Compounds*, 4th ed.; John Wiley: Singapore, 1981; p 113.
(29) Kaplan, S.; Conwell, E. M.; Richter, A. F.; MacDiarmid, A. G. *J. Am. Chem. Soc.* **1988**, *110*, 7647.

(30) Cao, Y.; Li, S.; Xue, Z.; Guo, D. *Synth. Met.* **1986**, *16*, 857.
(31) Euler, W. B. *Solid State Commun.* **1986**, *57*, 857.
(32) Stafstrom, S.; Bredas, J. L.; Epstein, A. J.; Woo, H. S.; Tanner, B. D.; Huang, W. S.; MacDiarmid, A. G. *Phys. Rev. Lett.* **1987**, *59*, 1464.
(33) Asturias, G. E.; MacDiarmid, A. G.; McCall, R. P.; Epstein, A. J. *Synth. Met.* **1989**, *29*, E157.
(34) Masters, J. G.; Sun, Y.; MacDiarmid, A. G.; Epstein, A. J. *Synth. Met.* **1991**, *41*, 715.
(35) Kumar, S. N.; Gaillard, F.; Bouyssoux, G.; Sartre, A. *Synth. Met.* **1990**, *36*, 111.
(36) Monkman, A. P.; Stevens, G. C.; Bloor, D. *J. Phys. D: Appl. Phys.* **1991**, *24*, 738.
(37) Clark, D. T.; Thomas, R. H. *J. Polym. Sci., Polym. Chem. Ed.* **1978**, *16*, 791.
(38) Salaneck, W. R.; Lundstrom, I.; Hjertberg, T.; Duke, C. B.; Conwell, E.; Paton, A.; MacDiarmid, A. G.; Somasari, N. L. D.; Huang, W. S.; Richter, A. F. *Synth. Met.* **1987**, *18*, 291.
(39) Menardo, C.; Nechtschein, M.; Rousseau, A.; Travers, J. P.; Hany, P. *Synth. Met.* **1988**, *25*, 311.
(40) Chan, H. S. O.; Ang, S. G.; Ho, P. K. H.; Johnson, D. *Synth. Met.* **1990**, *36*, 103.
(41) Chan, H. S. O.; Ho, P. K. H.; Tan, K. L.; Tan, B. T. G. *Synth. Met.* **1990**, *35*, 333.
(42) MacDiarmid, A. G.; Manohar, S. K.; Masters, J. G.; Sun, Y.; Weiss, H.; Epstein, A. J. *Synth. Met.* **1991**, *41*, 621.
(43) Muilenberg, G. E., Ed. *Handbook of X-ray Photoelectron Spectroscopy*; Perkin-Elmer Physical Electronics: Eden Prairie, MN, 1978.
(44) MacDiarmid, A. G.; Chiang, J. C.; Richter, A. F.; Epstein, A. J. *Synth. Met.* **1987**, *18*, 285.
(45) Wei, Y.; Hsueh, K. F. *J. Polym. Sci., Polym. Chem. Ed.* **1989**, *27*, 4351.
(46) Chan, H. S. O.; Teo, M. Y. B.; Khor, E.; Lim, C. N. *J. Them. Anal.* **1989**, *35*, 765.
(47) Chan, H. S. O.; Ho, P. K. H.; Tan, M. M.; Tan, K. L.; Tan, B. T. G.; Lim, Y. *K. Synth. Met.* **1989**, *31*, 95.
(48) Wang, S.; Wang, F.; Ge, X. *Synth. Met.* **1986**, *16*, 99.
(49) Wei, Y.; Jang, G. W.; Hsueh, K. F.; Scherr, E. M.; MacDiarmid, A. G.; Epstein, A. J. *Polymer* **1992**, *33*, 314.
(50) Wei, Y.; Tang, X.; Sun, Y.; Focke, W. *J. Polym. Sci., Polym. Chem. Ed.* **1989**, *27*, 2385.
(51) Lowry, H.; Richardson, K. S. *Mechanism and Theory in Organic Chemistry*, 2nd ed.; Harper and Row: New York, 1981; p 139.